Nuclear Physics B315 (1989) 419–435
North-Holland, Amsterdam

A FINITE SIZE ANALYSIS OF THE HEAVY QUARK POTENTIAL IN A DECONFINING MEDIUM

J. ENGELS[1], F. KARSCH[2] AND H. SATZ[1,3]

CERN, Geneva, Switzerland

Received 9 May 1988

From lattice studies of Polyakov loop correlations, we determine the potential for a static quark–antiquark pair in a thermal SU(2) gauge field system above the deconfinement temperature. We perform a high statistics, finite size analysis of the heavy quark potential. We investigate the functional form of the potential at intermediate distances and compare it to continuum perturbation theory predictions.

1. Introduction

The temperature dependence of the potential between a static quark and antiquark in a deconfining medium is of considerable interest for several reasons. The effect of such a medium on heavy quark bound states, in particular on the J/ψ, appears to provide an experimentally accessible signal for quark deconfinement in nuclear collisions [1]; a quantitative understanding of colour screening is necessary for these considerations [2]. In particular, the functional form of the potential at moderate distances $r \leqslant 1.0$ fm and temperatures $T \simeq 200$–300 MeV seems to be most relevant for the quantitative analysis of J/ψ bound state formation in the QCD plasma. In terms of the dimensionless quantity rT, we are thus mainly interested in the regime $0 \leqslant rT \leqslant 1.5$. A non-perturbative analysis is needed in this parameter range, as perturbative results are expected to become applicable only in the large-distance, high-temperature limit of the potential.

On a more theoretical level, asymptotic freedom implies that statistical QCD should at a sufficiently high temperature approach the perturbative limit. However, the well-known infra-red problems in finite-temperature perturbative expansions signal that above certain length scales non-perturbative effects will be of relevance even at very high temperatures. The presence of a non-vanishing screening length in the QCD plasma phase is in itself a manifestation of these non-perturbative effects.

[1] Universität Bielefeld, Fakultät für Physik, D-4800 Bielefeld 1, F.R. Germany.
[2] CERN, CH-1211 Geneva 23, Switzerland.
[3] Physics Department, Brookhaven National Laboratory, Upton, NY 11973, USA.

Through its definition as the zero momentum limit of the time component of the polarization tensor, the Debye mass $\mu(T)$ (i.e. the inverse screening length) is related to the asymptotic behaviour of the potential at $r \to \infty$. It has been calculated perturbatively only at high temperature, where the gauge coupling tends to zero. Recently it was noted that this does not necessarily reflect the behaviour of the potential at intermediate distances and temperatures [3]. Moreover, the perturbative definition of the Debye mass through the polarization tensor itself is not without problems, as this is a gauge invariant concept only in leading order. It even has been argued that higher order corrections may not be calculable in perturbation theory. These problems make the perturbative analysis of the heavy quark potential questionable [4, 5].

Unlike thermodynamic quantities such as the energy density, which shows perturbative behaviour in the deconfinement phase already close to T_c, the heavy quark potential led in first Monte Carlo studies to an unexpectedly large value for the Debye screening mass in the plasma phase [6, 7]. Also the functional form of the potential turned out not to be in agreement with perturbation theory for quite a large temperature range. This might hint toward a breakdown of perturbation theory, as speculated in ref. [5]. However, it could also indicate that on finite lattices it is much harder to reproduce the subtle long-distance properties of the plasma phase than the short-distance features, which give the main contribution to, for instance, the energy density [8]. In a recent paper [9] it was shown that for quite a large temperature interval above the deconfinement point, the heavy quark potential at intermediate distances does not lead to simple Debye screened Coulomb behaviour.

Although indications were found for the onset of perturbative behaviour at temperatures of the order of $10T_c$, the agreement turned out to be still quite poor. The analysis was performed for SU(3) gauge theory on a lattice of fixed size $12^3 \times 4$. Is such a lattice large enough to approximate continuum physics? Certainly at large distances we are sensitive to finite size effects. For instance, on the $12^3 \times 4$ lattice the potential is periodic around $rT = 1.5$ and thus at this distance will certainly be affected by the finite lattice size.

Here we want to analyze in detail the influence of the finite temporal (N_τ) and spatial (N_σ) extension of the lattice on the heavy quark potential. In order to be able to collect high statistics data, we work with the SU(2) gauge group on lattices of size $N_\sigma^3 \times N_\tau$ where N_σ varies between 4 and 24 and N_τ between 4 and 8; thus the smallest lattice used was 4^4 and the largest one was $24^3 \times 8$. We find that at high temperatures finite size effects in the potential $V(r, T)$ are well parametrized by

$$V(r, T) = V_\infty(r, T)\exp\left[-c(r, T)(N_\tau/N_\sigma)^3\right]; \tag{1}$$

close to T_c, the volume dependence seems to be more complicated. Thus the high-temperature behaviour appears to be closely related to the finite size corrections found for scattering states in massive scalar field theories [10], although in our case, a similar rigorous justification for the finite size behaviour is still missing at present. On the basis of the above formula we are, however, able to extract the potential in the infinite volume limit.

This paper is organized as follows. In sect. 2 we give a non-perturbative definition of the heavy quark potential at finite temperature, free of divergent self-energy terms. Sect. 3 deals with the volume dependence of the heavy quark potential in the deconfinement phase. We discuss the influence of finite size effects on the screening mass and perform a quantitative analysis of the volume dependence. Sect. 4 contains our conclusions.

2. The heavy quark potential

In lattice QCD, the potential for a static $q\bar{q}$ pair separated by a distance r is either obtained from the asymptotic behaviour of Wilson loops $W(R, S)$, $S \to \infty$, or from the correlation function $\langle L(0)L^+(R)\rangle$ for two Polyakov loops L, which are R lattice spacings a apart, i.e. $R = r/a$. It is this latter method which can be applied directly to the finite temperature situation and allows a general analysis of the temperature dependence of the heavy quark potential

$$\langle L(0)L^+(R)\rangle \sim \exp\left[-\beta V_{q\bar{q}}(r, T)\right]; \tag{2}$$

here $\beta = 1/T$ is the inverse temperature of the medium and

$$L(x) = \frac{1}{N}\mathrm{Tr}\prod_{i=1}^{N_\tau} U_{x,i}. \tag{3}$$

We assume an isotropic ($a_\sigma = a_\tau$) underlying lattice of size $N_\sigma^3 \times N_\tau$, with σ and τ designating space and temperature directions, respectively. The gauge group element $U_{x,i}$ is associated to the ith temperature link at the spatial site x; N specifies the colour group. The limit $R \to \infty$ of the correlation function leads to the deconfinement measure $\bar{L}$

$$\bar{L} = \lim_{R\to\infty} \langle L(0)L^+(R)\rangle^{1/2}, \tag{4}$$

where $\bar{L} = \langle L \rangle$ is the Polyakov loop expectation value with L defined as

$$L = (1/N_\sigma)^3 \sum_x L(x). \tag{5}$$

Since in pure gauge theory, confinement implies that $\lim_{r\to\infty} V(r, T) = \infty$ for

$T \leqslant T_c$, $\bar{L}$ in this case constitutes a genuine order parameter, associated to a global Z_N symmetry of the lagrangian [11].

It is well known that the definitions (2) and (4) for the heavy quark potential and the order parameter do not lead to finite physical expressions in the continuum limit. Both expressions still contain self-energy terms which lead to divergences as the lattice cut-off $1/a$ is removed [12]; thus the potential $V_{q\bar{q}}(r, T)$ in eq. (2) consists of the actual $q\bar{q}$ interaction part, $V(r, T)$, and a self-energy term for the q and $\bar{q}$ charges, $V_0 \sim -g^2/r$, which diverges at short distances. On the lattice, $\beta = N_\tau a$, and the shortest distance is the lattice spacing $r = a$, so that

$$\langle L(0) L^+(R) \rangle \sim \exp[-\beta V(r, T) - \text{const.}\, g^2 N_\tau] . \tag{6}$$

As a consequence of eq. (6), both $\langle L(0) L^+(R) \rangle$ and $\bar{L}$ are not lattice-size independent; they vanish exponentially as N_τ is increased. There have been attempts [13] to remove this lattice size dependence by dividing out the weak-coupling limit of $\bar{L}$

$$\bar{L}_{\text{wc}} = 1 + c_1(N_\tau, N_\sigma) g^2 + c_2(N_\tau, N_\sigma) g^4 + O(g^6) , \tag{7}$$

and considering $\bar{L}_{\text{phys}} = \bar{L}/L_{\text{wc}}$ as the physical (and hence scaling) order parameter. However, the N_τ dependence of $\bar{L}_{\text{wc}}$ requires the inclusion of ever higher orders in g^2 with increasing N_τ, and hence such a method does not provide a general solution.

To obtain a physically meaningful definition of the heavy quark potential, we have to eliminate the self-energy contributions in a non-perturbative way. This can be done by looking at differences of the potential only. Just as one forms Creutz ratios to eliminate the perimeter and corner singularities in the definition of the string tension, we may consider ratios of Polyakov loops as physical observables

$$PL(R_1, R_2) = \langle L(0) L^+(R_1) \rangle / \langle L(0) L^+(R_2) \rangle . \tag{8}$$

These quantities are directly related to the difference of the potential at distance r_1 and r_2; the additative self-energy terms are now eliminated

$$[V(r_1, T) - V(r_2, T)]/T = -\ln[PL(R_1, R_2)] . \tag{9}$$

In the following we will consider a special case: we normalize the potential to be zero at infinity

$$V(r, T)/T = -\ln[PL(R, \infty)] . \tag{10}$$

In practice, we have to specify more carefully what we mean by $PL(R, \infty)$, since on any finite lattice $\bar{L}$ will become zero by "spin flips". We thus define more precisely [7]

$$PL(R,\infty) \equiv \langle L(0)L^{+}(R)\rangle / \langle |L|\rangle^{2}. \tag{11}$$

This definition coincides with that of eq. (8) when $N_\sigma \to \infty$, and $R_2 \to \infty$. As these quantities are now free of self-energy divergences, they should become asymptotically independent of the temporal lattice size N_τ. They will, however, still contain the usual size effects, which we will discuss together with the Monte Carlo data in sect. 3.

In order to compare measurements of the potential on lattices with different N_τ, we have to ensure that the temperature stays constant and that the potential is measured for the same physical separation. On a given lattice, one studies the variation of $V(r,T)$ with r at fixed temperature, i.e. at fixed coupling g^2; as already mentioned, the separation r is measured in units of the lattice spacing $a(g^2)$,

$$R = r/a = 1, 2, \ldots, N_\sigma/2. \tag{12}$$

The upper limit $N_\sigma/2$ arises from periodic spatial boundary conditions. If we now want to measure the correlation at a fixed temperature $T^{-1} = N_\tau a(g^2)$ on lattices with different N_τ, then the g^2 values associated to this temperature will of course depend on N_τ. As a result, a given $q\bar{q}$ separation of e.g. two lattice spacings then corresponds to a different physical separation distance for each N_τ. To obtain a basis for comparing results from different lattices, we consider the dimensionless quantity $V(r,T)/T$, defined through eq. (11), at fixed T as a function of the dimensionless variable $rT = R/N_\tau$. For fixed T the potential will then still depend on the ratio N_σ/N_τ, even if both N_σ and N_τ are large. By keeping N_σ/N_τ fixed and taking the limit $N_\sigma \to \infty$, $N_\tau \to \infty$ we simulate continuum physics at finite temperature in a finite box with volume V and temperature T related by $V^{1/3}T = N_\sigma/N_\tau$. The infinite volume limit is then reached for $N_\sigma/N_\tau \to \infty$, $N_\tau \to \infty$, while temperature $T = 1/N_\tau a(g^2)$ is kept fixed.

In order to study the scaling behaviour of the heavy quark potential we thus have to ensure that the temperature stays constant when we change the lattice size, and we have to control possible effects related to the small finite extension of the lattice in temporal and spatial directions. The variation of the temperature as a function of g^2 is a problem close to T_c, where we are not yet in the asymptotic scaling regime, at least not for small values of N_τ. To avoid this difficulty in the beginning, we have first analyzed the potential at very high temperatures, where we expect the asymptotic scaling relation to be valid; it then allows us to calculate the temperature as a function of g^2. The temperature was chosen to be $T/\Lambda_L \simeq 250$; on the basis of results for $N_\tau = 3$–5, this corresponds to $T/T_c \simeq 6$, where T_c is the deconfinement temperature [13].

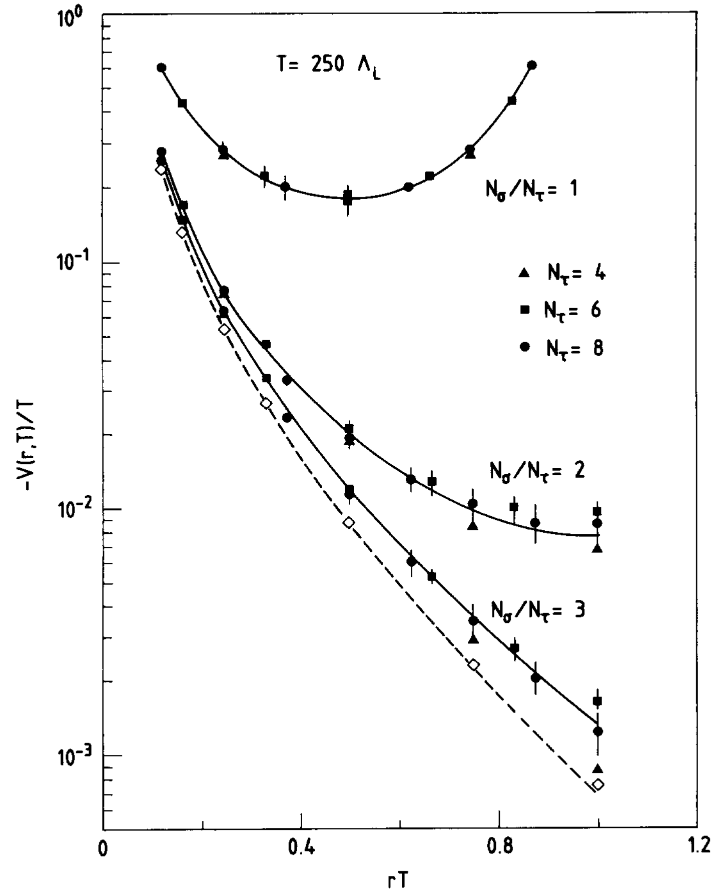

Fig. 1. The interquark potential $-V(r,T)/T$ versus rT at fixed temperature $T = 250\Lambda_L$. The couplings used in the simulation are $\beta = 2.988$ ($N_\tau = 4$), $\beta = 3.147$ ($N_\tau = 6$) and $\beta = 3.26$ ($N_\tau = 8$). The dashed curve gives the potential extrapolated to infinite volume.

For large enough N_σ and N_τ we expect the potential to be a function of N_σ/N_τ only. In fig. 1 we show results for the potential obtained for $N_\sigma/N_\tau = 1, 2, 3$ and $N_\tau = 4$, 6 and 8. This figure summarizes results from 9 different lattices ranging in size from 4^4 to $24^3 \times 8$. On each of these lattices we performed 100000 iterations, except for the smallest and largest ones, where we used 200000 and 50000, respectively. Measurements of Polyakov loop correlation functions were carried out every 10th iteration. Errors were calculated by dividing the data sample in 10 blocks of equal size. On these blocks, the heavy quark potential was calculated using eqs. (10) and (11). The error was then determined as the statistical error of these 10 independent measurements of the potential.

A more detailed discussion of our fits will be given in sect. 3. Here we only want to note that we do indeed find universal curves for all N_τ at fixed N_σ/N_τ; the scattering of results from different N_τ is well within statistical errors. The prescription for the elimination of unphysical self-energy terms given in eq. (11) thus seems to work quite well. We also see from fig. 1 that the potential depends strongly on the ratio N_σ/N_τ. In particular for $rT \geqslant 0.5$ this was to be expected, as we start feeling the periodicity of the lattice. Let us now try to analyze these finite size effects.

3. The volume dependence of the potential

The heavy quark potential in the deconfinement phase is expected to be of the generic Debye screened form

$$\frac{V(r,T)}{T} = -\frac{\alpha(T)}{(rT)^d} e^{-\mu(T)r}, \tag{13}$$

with a temperature-dependent coupling α and a screening mass μ. High-temperature perturbation theory predicts $d=2$ as the power of the $1/r$ term in eq. (13). In perturbation theory, the screening mass $\mu = 2m_\mathrm{D}$ is usually defined as the zero momentum limit of the zeroth component of the vacuum polarization tensor

$$m_\mathrm{D}^2 = \lim_{k\to 0} \Pi_{00}(0, \boldsymbol{k}) = \tfrac{1}{3} N g^2(T) T^2. \tag{14}$$

Therefore, a simple Debye screened potential of the form given by eq. (13) is predicted only in the large distance (zero momentum) limit. Finite momentum corrections to the polarization tensor are found to be negative [14] and of the same order in g^2. At intermediate distances one would thus expect [3] deviations from the simple Debye form given by eq. (13). In particular, one would expect a smaller screening mass in this regime, and consequently also in a finite volume. This is indeed what was found in perturbative calculations on a finite lattice [15]. A weak coupling analysis of the QCD vacuum polarization tensor at finite temperature [15, 16], shows that the Debye mass is smaller on finite lattices and scales with VT^3 on large lattices. For large N_σ/N_τ one recovers the continuum result in a finite box given by

$$\frac{\mu^2}{\mu_\infty^2} = \frac{3}{2}\frac{1}{VT^3}\sum_{n_i}{}' \sinh^2\left[\frac{\pi}{V^{1/3}T}\sqrt{n_1+n_2+n_3}\right], \qquad n_i = 0, \pm 1, \pm 2, \dots . \tag{15}$$

Here Σ' indicates that the zero-mode contribution is left out in the summation. The volume dependence of the perturbative continuum Debye mass given by eq. (15) is shown in fig. 2.

We expect this to be the dominant source of finite volume effects at high temperature. Close to T_c, however, there is a competing mechanism for finite size effects, related to the large correlation length near deconfinement. With increasing lattice size, the correlation length tends to increase and thus would lead to a lower

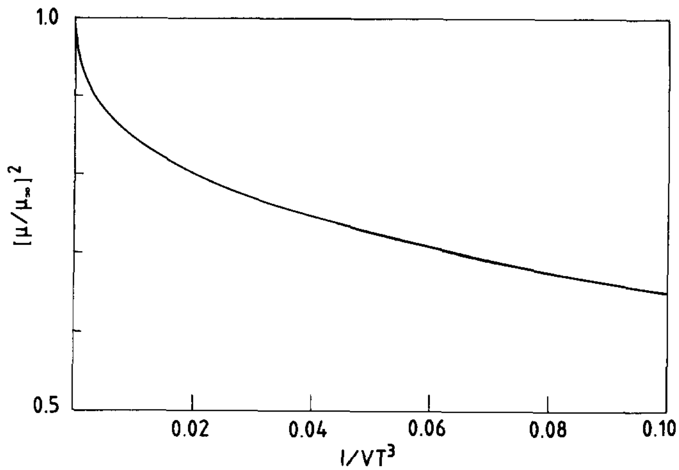

Fig. 2. Volume dependence of the Debye mass from continuum perturbation theory in a finite box. Shown is the square of the ratio μ/μ_∞ between the Debye mass in a finite and in an infinite volume, as function of $1/VT^3$.

screening mass. As the deconfinement transition for SU(2) is second order, the correlation length actually diverges at T_c [7]. This may become the dominant source of finite volume dependence close to T_c.

In order to study the dependence on $N_\sigma/N_\tau = V^{1/3}T$ in more detail, we have calculated the potential for $N_\tau = 6$ and various spatial lattice sizes. The restriction to one value of N_τ is justified, since we saw in sect. 2 that the potential depends only on N_σ/N_τ. Our analysis was performed for two values of the temperature, $T/\Lambda_L \simeq 55$ ($\beta = 2.567$) and $T/\Lambda_L \simeq 250$ ($\beta = 3.147$). In units of the deconfinement temperature, this corresponds to $T/T_c \simeq 1.45$ and $T/T_c \simeq 6$, respectively. In fig. 3, we show the heavy quark potential for various intermediate values of N_σ/N_τ and fixed N_τ. Again we have performed 100000 iterations on each lattice and the error analysis was carried out as described above. We notice that even for rather large values of the ratio N_σ/N_τ, finite size effects are clearly visible in the potential at both temperatures. It seems, however, that the asymptotic infinite volume limit is reached faster close to T_c. To study the systematics of the observed finite volume effects, we show in fig. 4 $V(r,T)/T$ at fixed distance rT as a function of $(N_\tau/N_\sigma)^3$. This suggests a parametrization of the finite volume dependence in the form given by eq. (1); for the logarithms of the potential we find a linear dependence on $(N_\tau/N_\sigma)^3 = 1/VT^3$

$$\ln[V_\infty(r,T)/T] = \ln[V(r,T)/T] - c(r,T)/VT^3. \tag{16}$$

However, while this linear relation seems to hold at $T/\Lambda_L \simeq 250$ already for moderate sizes of the volume, $VT^3 > 4$, it appears to set in much later close to T_c.

Using the above ansatz, we can extrapolate our Monte Carlo data for the potential to infinite lattice size. Fits for some values of rT are also shown in fig. 4. The fit parameters $V_\infty(r,T), c(r,T)$ for both temperatures are summarized in table 1. We note that $c(r,T)$ is smaller close to T_c, which means that finite volume corrections are indeed smaller here. It is also apparent that the slope parameter $c(r,T)$ increases with increasing rT. Indeed one would expect that $c(r,T)$ is directly proportional to rT, if the finite volume corrections for the potential are mainly due to a volume dependence of the screening mass μ. In this case eq. (16) states that finite volume corrections to the screening mass are porportional to $1/V$. For a potential of the form given by eq. (13) one would then deduce from eq. (16)

$$\frac{\mu_\infty}{T} = \frac{\mu}{T} + \frac{\bar{c}(T)}{VT^3}, \tag{17}$$

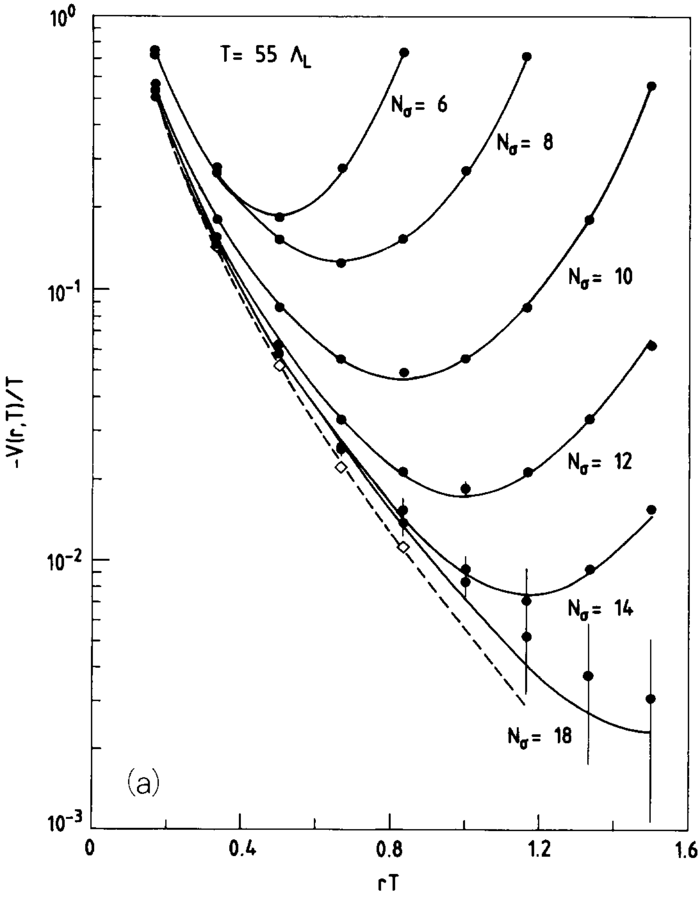

Fig. 3. As in fig. 1, but for fixed $N_\tau = 6$ and various values of N_σ. Fig. 3a shows results for $T = 55\Lambda_L$ ($\beta = 2.567$) and fig. 3b for $T = 250\Lambda_L$ ($\beta = 3.147$).

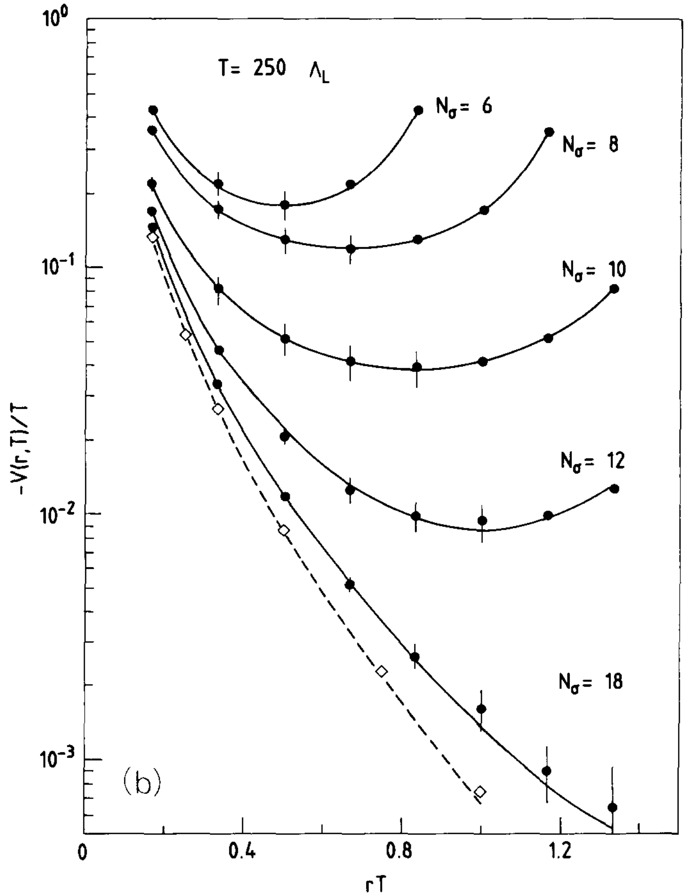

Fig. 3 (continued).

where $\bar{c}(T) = c(r, T)/rT$. From table 1 we find that, indeed, this relation holds quite well at $T/\Lambda_L \simeq 250$. We obtain at this temperature

$$\bar{c}(T) = 13.8 \pm 0.4 \quad \text{at} \quad T/T_c \simeq 6 . \tag{18}$$

This simple rT dependence of the finite volume corrections, however, does not seem to hold close to T_c. This situation was in fact expected and reflects the more complicated structure due to the competing mechanisms for finite volume effects discussed above. In any case $c(r, T)$ is clearly positive and increasing with rT at both temperatures. This leads to a steeper potential decrease in a larger volume. We thus conclude that at least for temperatures larger than 1.5 T_c finite volume effects tend to decrease the effective screening mass.

We now want to perform a more quantitative analysis of the potentials obtained in sects. 1 and 2. We will try to extract the effective screening mass both from fits to the potential as well as from ratios of the potential at subsequent lattice sites. We would like to stress that we distinguish between an effective screening mass characterizing the exponential decay of the potential at intermediate distances and the actual Debye mass defined through the asymptotic behaviour of the potential at large distances.

In order to analyze the functional form of the potential for $rT \leqslant 1.0$ in more detail, we fit the potential using the general form (13). We thus allow an arbitrary power d in the "Coulomb term" and assume an exponential decay characterized by an effective screening mass μ for this range of rT values. In the actual fit we, of course, take into account the periodicity of our lattices. Let us first analyze the potential at $T \simeq 250\Lambda_L$ shown in fig. 1. The results of a three-parameter χ^2-fit based

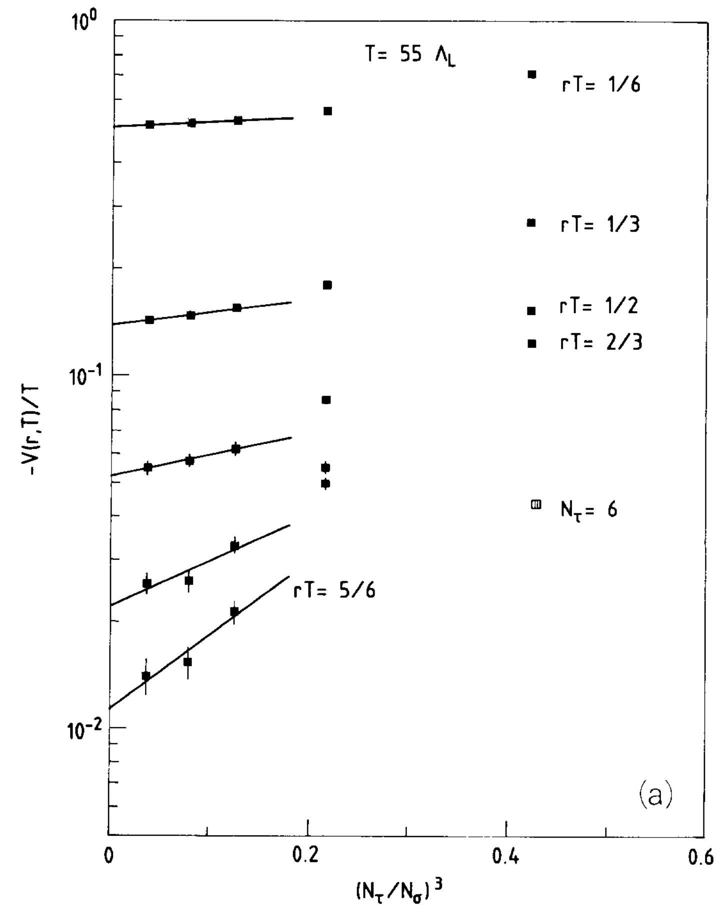

Fig. 4. The interquark potential $-V(r,T)/T$ versus $(N_\tau/N_\sigma)^3$ for various values of rT at $T = 55\Lambda_L$ (fig. 4a) and at $T = 250\Lambda_L$ (fig. 4b). The solid lines are fits to the data using the form (16). The dashed line in fig. 4b gives the extrapolation of our data at $rT = 1$ using eq. (16) with $c(r,T) = 13.8$.

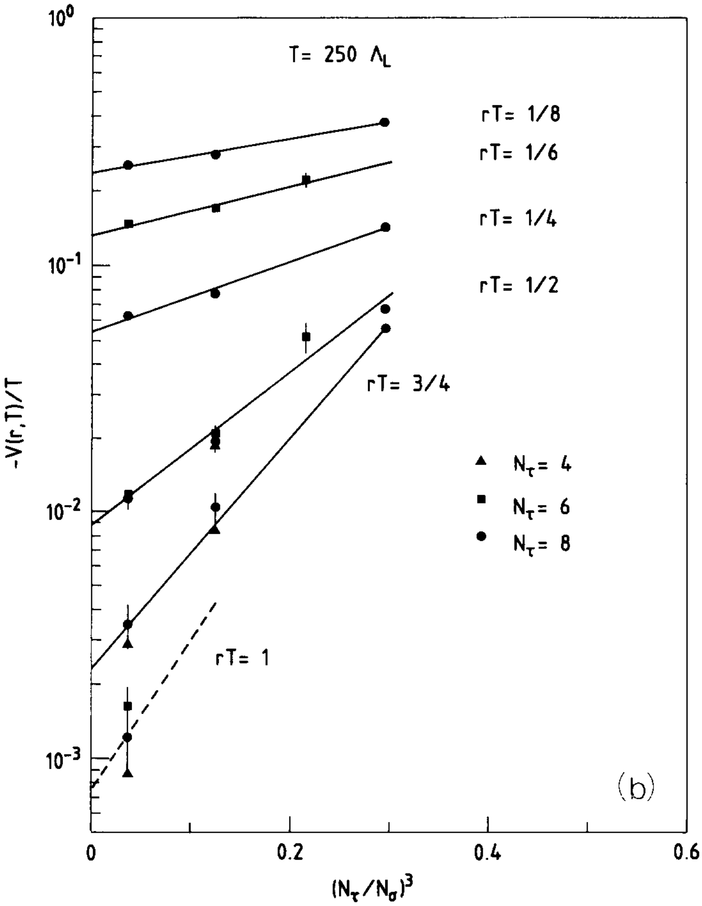

Fig. 4 (continued).

on eq. (13) are summarized in table 2. We note that although the fits are based on data points from three independent data samples (three different N_τ values), the data for fixed N_τ are strongly correlated. The errors quoted in the table are thus to be taken with some caution. The power d we find from the fit does not agree with the value $d = 2$ expected from perturbation theory; it is, however, consistent with our earlier result for the heavy quark potential in SU(3) gauge theory [9].

The fits indicate that the screening mass increases with increasing volume. The deviation between our largest lattices, with $N_\sigma/N_\tau = 3$, and the infinite volume extrapolation is about 20%. This result is in good agreement with the extrapolation formula, eq. (17), which would give $\mu_\infty/T = 2.8 \pm 0.1$. We thus find indeed that finite volume corrections mainly lead to a modification of the screening mass.

Further information on the volume dependence of the screening mass can be obtained from the data shown in fig. 3. Due to the fewer number of points we did

TABLE 1
Fit parameters for the infinite volume extrapolation shown in fig. 4

rT	$T=55\Lambda_L$ $V_\infty(r,T)$	$T=55\Lambda_L$ $c(r,T)$	$T=250\Lambda_L$ $V_\infty(r,T)$	$T=250\Lambda_L$ $c(r,T)$
1/8	0.2346	1.5790	—	—
1/6	0.1321	2.2403	0.5007	0.3404
1/4	0.05348	3.2425	—	—
1/3	0.02679	4.9923	0.1384	0.8448
1/2	0.008662	7.1997	0.05192	1.3931
3/4	0.002282	10.7125	—	—
2/3	—	—	0.02206	2.9670
5/6	—	—	0.01124	4.8586

TABLE 2
Parameters for the fits shown in fig. 1 ($T=250\Lambda_L$)

N_σ/N_τ	α	d	μ/T
1	0.0386	1.30(1)	0.13(2)
2	0.0085	1.72(1)	0.81(3)
3	0.0127	1.58(1)	2.30(8)
∞	0.0119	1.61(1)	2.87(20)

not perform a three-parameter fit here, but rather fixed the power d in eq. (19) to the value obtained from a three-parameter fit on our $18^3 \times 6$ lattices. Best fits were obtained for $d \simeq 1.2$ at $T=55\Lambda_L$ and $d \simeq 1.6$ at $T=250\Lambda_L$. We then performed two parameter χ^2-fits for the smaller lattices. The results are summarized in table 3 for both temperatures. Again this shows that the volume dependence is weaker close to T_c, although the screening mass still rises with increasing volume size.

TABLE 3
Parameters for the fits shown in fig. 3

N_σ/N_τ	$T=55\Lambda_L$ α	$T=55\Lambda_L$ μ/T	$T=250\Lambda_L$ α	$T=250\Lambda_L$ μ/T
1.00	0.1198	2.14	0.0178	−1.01
1.33	0.1042	1.47	0.0147	−1.14
1.67	0.0879	1.85	0.0113	−0.29
2.00	0.0895	2.34	0.0111	0.95
2.33	0.0923	2.59	—	—
3.00	0.0907	2.58	0.0120	2.21
∞	0.0936	2.83	0.0121	2.90

The screening mass determined in our fits characterizes the behaviour of the potential at relatively short distances, $rT \leqslant 1.0$. In order to clarify its relation to the actual Debye mass at large distances, we define R-dependent screening masses through ratios of the potential at distances separated by one lattice unit. The effective screening mass $\mu_{R,d}$ at distance $R = r/a$ for fixed value of d is then defined through [9]

$$\frac{V(R-1,T)}{V(R,T)} = \frac{(R-1)^{-d}\exp[-\mu_{R,d}(R-1)] + (N_\sigma - R+1)^{-d}\exp[-\mu_{R,d}(N_\sigma - R+1)]}{R^{-d}\exp(-\mu_{R,d}R) + (N_\sigma - R)^{-d}\exp[-\mu_{R,d}(N_\sigma - R)]}. \tag{19}$$

Results for $d = 1.0$, 1.5 and 2.0 are shown in fig. 5 for our largest lattice, $24^3 \times 8$ at $T/\Lambda_L \simeq 250$. For large rT the masses should become independent of d. We see that effective masses extracted for $d = 1$ and 2 give upper and lower bounds for the screening masses in the $rT \to \infty$ limit. With increasing rT these bounds become more stringent. For instance at $rT = 1$ we find

$$2.0 < \mu/T < 3.0, \tag{20}$$

which is in good agreement with our fits.

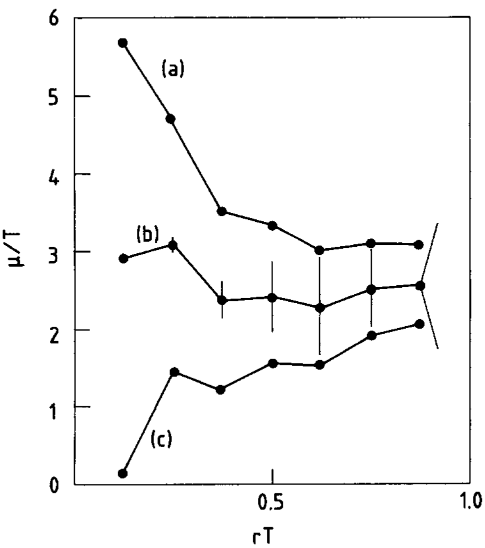

Fig. 5. Effective screening masses $\mu_{R,d}$ for $d = 1$ (a), 1.5 (b) and 2 (c) versus $R = r/a$ on a $24^3 \times 8$ lattice at $T = 250\Lambda_L$ ($\beta = 3.26$). For clarity we only show errors on curve (b), those on (a) and (c) are similar. Lines are drawn to guide the eye.

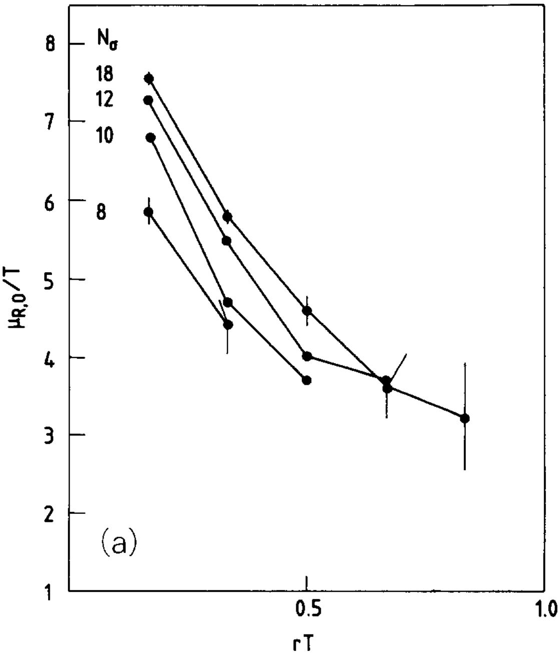

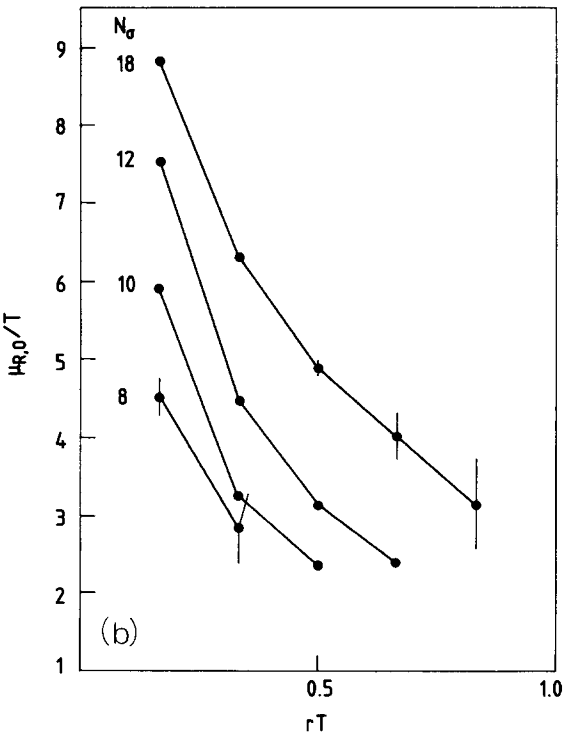

Fig. 6. Volume dependence of the effective screening masses $\mu_{R,d}$ for $d=0$ and various values of N_σ/N_τ. Results shown are for $N_\tau=6$ and $T=55\Lambda_L$ (fig. 6a) and $T=250\Lambda_L$ (fig. 6b). For clarity we only show errors for the smallest and largest lattice. Lines are drawn to guide the eye.

The above analysis of the screening mass has the advantage that it does not have to rely on any fits. This way we can also analyze the finite volume effects on the Debye mass. In fig. 6 we show $\mu_{R,d}$ for $d=0$ for various lattice sizes. We clearly see that at fixed distance the screening mass increases with increasing size of the spatial volume, while for a given volume the mass decreases with increasing distance. Again we notice that the volume dependence is stronger at higher temperature. In addition also the r-dependence is stronger, indicating that the effective power for the "Coulomb term" at short distances is larger at higher temperature. This is in agreement with our results from the three-parameter fits. In general we find that the effective screening masses extracted from a three-parameter fit with a potential of the form given by eq. (19) are in good agreement with masses extracted from potential ratios at large distances.

4. Conclusions

We have studied the static heavy quark potential in a finite volume. We find that self-energy terms can be eliminated, if an appropriate normalization of the potential with Polyakov loop expectation values is used. This leads to a scaling potential $V(r, T)$, which depends on the volume only through the dimensionless quantity $V^{1/3}T = N_\sigma/N_\tau$.

At distances $rT \leqslant 1.0$, the infinite volume limit of the potential is well approximated by lattices with $N_\sigma/N_\tau = 3$. This potential can be described by the phenomenological form $V(r,T)/T = [\alpha(T)/(rT)^d]\exp[-\mu(T)r]$. For temperatures close to T_c we have $d \simeq 1.0$, while for higher temperatures d increases, at $T/T_c \simeq 6$, $d \simeq 1.6$. It thus does not reach the perturbation theory prediction $d=2$ in the parameter range considered here ($T/T_c \leqslant 6$, $rT \leqslant 1.5$).

We find that finite volume corrections to the potential mainly lead to a modification of the screening mass, describing the exponential decrease of the potential at intermediate distances. For the temperature range studied by us, i.e. $T/T_c \geqslant 1.5$, finite volume effects lead to an increase of the screening mass with increasing lattice size. However, these finite volume effects seem to be larger at high temperature than close to T_c. One would in fact expect that close to a second-order phase transition finite volume effects work the opposite way, since then the correlation length is truncated on finite lattices but tends to diverge in the infinite volume limit at T_c. A further analysis of the volume dependence of the screening mass even closer to T_c would therefore be of interest and could lead to a different volume dependence, once the correlation length becomes larger than the dimension of the system.

The Monte Carlo simulations were performed on the new Crays X-MP/48 at the HLRZ in Jülich and at CERN. One of us (F.K.) would like to thank K. Kajantie for helpful discussions.

References

[1] T. Matsui and H. Satz, Phys. Lett. B178 (1986) 416
[2] F. Karsch, M.T. Mehr and H. Satz, Z. Phys. C37 (1988) 617
[3] C. Gale and J. Kapusta, Phys. Lett. B198 (1987) 89
[4] S. Nadkarni, Phys. Rev. D33 (1986) 3738
[5] S. Nadkarni, Phys. Rev. D34 (1986) 3904
[6] T.A. DeGrand and C.E. DeTar, Phys. Rev. D34 (1986) 2469
[7] K. Kanaya and H. Satz, Phys. Rev. D34 (1986) 3193
[8] F. Karsch, Z. Phys. C38 (1988) 147
[9] N. Attig, F. Karsch, B. Petersson, H. Satz and M. Wolff, Phys. Lett. B209 (1988) 65
[10] M. Lüscher, Commun. Math. Phys. 104 (1986) 177; 105 (1986) 153
[11] B. Svetitsky, Phys. Rep. 132 (1986) 1
[12] R.V. Gavai, F. Karsch and H. Satz, Nucl. Phys. B220[FS8] (1983) 481
[13] J. Engels, J. Jersak, K. Kanaya, E. Laermann, C.B. Lang, T. Neuhaus and H. Satz, Nucl. Phys. B280[FS18] (1985) 254;
J. Engels, J. Fingberg and M. Weber, Bielefeld preprint, BI-TP/88-6 (February 1988)
[14] K. Kajantie and J. Kapusta, Ann. Phys. 160 (1985) 513
[15] H.Th. Elze, K. Kajantie and J. Kapusta, Nucl. Phys. B304 (1988) 832
[16] U. Heller and F. Karsch, Nucl. Phys. B251[FS13] (1985) 254